ELSEVIER

Catalysis Today 32 (1996) 285–290

CATALYSIS TODAY

# Ammoxidation of methylaromatics over vanadium phosphate catalysts
# II. Catalyst formation, active sites and reaction mechanism

H. Berndt [a,*], K. Büker [a], A. Martin [a], S. Rabe [a], Y. Zhang [a], M. Meisel [b]

[a] *Institut für Angewandte Chemie Berlin-Adlershof e.V., Rudower Chaussee 5, D-12489 Berlin, Germany*

[b] *Humboldt Universität zu Berlin, Institut für Anorganische und Allgemeine Chemie, Hessische Straße 1-2, D-10115 Berlin, Germany*

**Abstract**

The interactions of $VOHPO_4 \cdot 0.5H_2O$ and $(VO)_2P_2O_7$ with the ammoxidation feed and the single components such as ammonia, oxygen, water and component mixtures were studied in detail using XRD and temperature-programmed reaction spectroscopy. The aim of this work was to improve the knowledge of the formation of the active phases or active sites of the catalysts from their precursors under the condition of the ammoxidation reaction. Similar catalytic properties of various applied VPO materials were discussed in terms of the presence of similar structure elements (domains of adjacent edge-sharing $VO_6$ octahedra-units and P-O-$NH_4$ groups).

*Keywords:* Ammoxidation; Methylaromatics; Vanadium phosphate catalysts; Catalyst formation; Active sites; Reaction mechanism

## 1. Introduction

Vanadium phosphates (VPO) of different structures are suitable precursors of very active and selective catalysts for the oxidation of $C_4$-hydrocarbons to maleic anhydride (e.g. [1]) as well as for the ammoxidation of methylaromatics and heteroaromatics to the corresponding nitriles [2,3]. Among a wide variety of VPO materials oxovanadium(IV) phosphate hemihydrate $VOHPO_4 \cdot 0.5H_2O$ and oxovanadium(IV) diphosphate $(VO)_2P_2O_7$ play an outstanding role. The interaction of various VPO materials, such as $VOHPO_4$, $VOHPO_4 \cdot 0.5H_2O$ and α- or β-$VOPO_4$ with the ammoxidation feed is accompanied by structural transformations of the precursor. This transformation leads to a product, consisting mainly of a new $NH_4^+$-containing VPO structure (NVPO), being α-$(NH_4)_2[(VO)_3(P_2O_7)_2]$ as revealed by XRD [3,4]. Interestingly, NVPO generated on-stream shows an activity and nitrile selectivity, being comparable with those of $(VO)_2P_2O_7$ that has a completely different bulk structure. From this result the question arises whether the ammoxidation of methylaromatics is either completely insensitive to the structure of the various VPO catalysts or whether the catalysts possess one common structure element after formation under ammoxidation conditions which is responsible for the catalytic properties. Clearly, a better

* Corresponding author.


*PII* S0920-5861(96)00079-X

understanding of the reaction mechanism needs detailed investigations of the catalyst formation process and of the generation of the active sites under catalytic conditions.

This paper presents current results concerning the formation process of α-$(NH_4)_2[(VO)_3(P_2O_7)_2]$ in relation to the surface reactions of $(VO)_2P_2O_7$. The interaction of the feed components of the ammoxidation of methylaromatics with $(VO)_2P_2O_7$ and $VOHPO_4 \cdot 0.5H_2O$ was studied by XRD and temperature-programmed reaction spectroscopy (TPRS). Additionally, these results are compared with the catalytic properties of various VPO catalysts.

## 2. Experimental

### 2.1. Catalysts

$VOHPO_4 \cdot 0.5H_2O$ used as precursor was transformed to $(VO)_2P_2O_7$ under nitrogen [5] or to α-$(NH_4)_2[(VO)_3(P_2O_7)_2]$ (abbreviation: $NVPO_{aox}$) under ammoxidation feed [2,6]. The generation of $NVPO_{aox}$ must be accompanied by the formation of an additional, XRD-amorphous vanadium rich oxidic phase, as revealed by the change of the V/P ratio in the educt (V/P = 1) and the crystalline part of the product (V/P = 0.75), being detectable by XRD [see Eq. (1) below]. Pure α-$(NH_4)_2[(VO)_3(P_2O_7)_2]$ (abbreviation: $NVPO_{syn}$) was prepared by heating a mixture, containing $V_2O_5$ (0.055 mol), $(NH_4)_2HPO_4$ (0.88 mol) and a small amount of inoculating crystals at 598 K for 2.5 h in air. A light green powder was obtained after the raw sample had been eluted with water and dried in air (see also [7]). In addition, mixtures of $NH_4VO_3$ and $NVPO_{syn}$ were prepared either by mechanical mixing ($NVPO_{syn/m}$) or by impregnation of $NVPO_{syn}$ with aqueous $NH_4VO_3$ solution ($NVPO_{syn/i}$). The molar amount of vanadium added to $NVPO_{syn}$ was comparable to the amount of the vanadium of the additional oxidic phase in $NVPO_{aox}$.

### 2.2. Methods

XRD patterns of precursor transformation products were recorded with a Stoe automatic transmission powder diffractometer (STADIP) using Cu $K_{\alpha 1}$ radiation [7]. TPRS was carried out using the dynamical catalyst characterization system AMI-1 (Altamira Instruments) coupled to a quadrupole mass spectrometer QMG-420C (Balzers) [5]. A micro tube reactor coupled with an on-line GC was applied for catalytic testing. The ammoxidation of toluene to benzonitrile was used as a model reaction [6].

## 3. Results and discussion

Recently, from TPRS, FTIR and EPR results on redox interactions/reactions of $NH_3$ and/or $O_2$ we concluded to the formation of a defined surface at the crystalline $(VO)_2P_2O_7$ bulk [5]. But no phase transformation could be detected. Certainly, this surface formation proceeds also under ammoxidation conditions. The edge-sharing $VO_6$ octahedra-units ($[V_2O_{10}]$) of the $(VO)_2P_2O_7$ are involved in a dynamical equilibration of oxidized and reduced vanadium surface species connected with the generation and disappearance of Brønsted as well as Lewis acid sites. A mechanism of the ammoxidation reaction with benzaldehyde-like surface intermediates and $NH_4^+$ as N-insertion source was derived from temporal-analysis-of-products (TAP) and FTIR results [8]. Transient measurements with $^{15}NH_3$-containing feed pulses in the TAP reactor revealed that $NH_4^+$ ions can act as N-insertion sites. Adsorption/reaction of the single ammoxidation feed components and of possible intermediates pointed to a reaction pathway via formation of benzaldehyde.

In contrast, the interaction of $VOHPO_4 \cdot 0.5H_2O$ with the ammoxidation feed ($NH_3$, air, water vapor and, for example, toluene) revealed a total structural transformation, generating $NVPO_{aox}$. Fig. 1 and the corresponding XRD

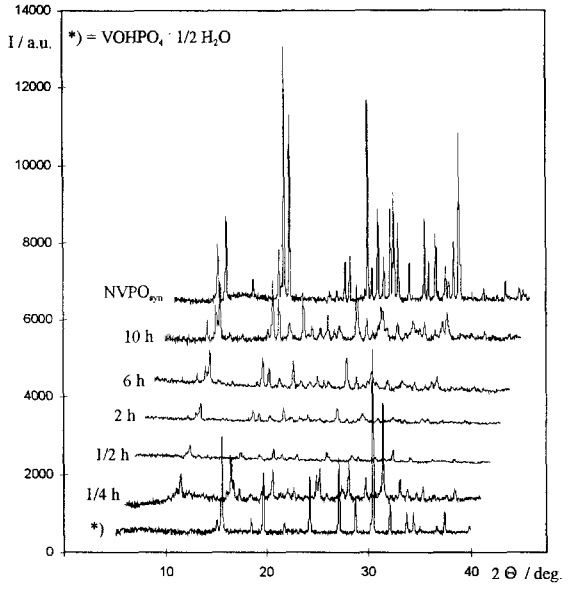


Fig. 1. XRD patterns of the precursor $VOHPO_4 \cdot 0.5H_2O$, of catalyst samples obtained after different periods of formation time under feed of the toluene ammoxidation at 673 K and of $NVPO_{syn}$.

data of Table 1 reflect the formation process of $\alpha$-$(NH_4)_2[(VO)_3(P_2O_7)_2]$, being isostructural to the corresponding potassium compound [7]. Considering the change of the V/P ratios, the following reaction [Eq. (1)] can be formulated:

$$VOHPO_4 \cdot 0.5H_2O + NH_3/O_2/H_2O \Rightarrow \alpha\text{-}(NH_4)_2[(VO)_3(P_2O_7)_2] + V_xO_y \quad (1)$$

Potentiometric titration of the transformation product showed a mean vanadium valence of 4.11, resulting from a ca. 50% $V^V$-portion of the XRD-amorphous phase $V_xO_y$. Therefore, it seems possible to consider the $V_xO_y$ phase as a mixed valent vanadium oxide. A deepened characterization by FTIR and Raman spectroscopy and comparison with spectra of various defined vanadium oxides could not yet reveal the structure of this phase [7]. Therefore, thermoanalytical investigations of $NVPO_{syn}$, $NVPO_{aox}$ and $NVPO_{syn/m}$ were carried out to obtain more knowledge about the properties of $V_xO_y$.

The ion current profiles of the temperature-programmed transformation reaction of $NVPO_{syn}$ and $NVPO_{aox}$ in a He flow are shown in Fig. 2. $NVPO_{syn}$ as well as $NVPO_{aox}$ revealed a liberation of $H_2O$ ($m/e$ 18) and $NH_3$ ($m/e$ 15), both starting at 673 K. However, the main part of $NH_3$ was desorbed between 773 and 873 K, whereas $H_2O$ was liberated up to 923 K. The double peak curve of water liberation clearly observed in the case of $NVPO_{syn}$ could be interpreted as a stepwise condensation reaction via amido groups-containing materials, presumably. The following reaction [Eq. (2)] can be formulated on basis of a quantitative evaluation of the amounts of $NH_3$ and $H_2O$ and on the elemental analysis of the solid product ($V_{theor.} = 29.05$ wt%, $V_{exp.} = 29.07$ wt%; $N_{theor.} = 1.77$ wt%, $N_{exp.} = 1.82$ wt%; $H_{exp.} = 0$ wt%):

$$3\alpha\text{-}(NH_4)_2[(V^{IV}O)_3(P_2O_7)_2] \Rightarrow V_9^{IV}O_{45}P_{12}N_2 + 6H_2O + 4NH_3 \quad (2)$$

However, by comparison with recent results [9] it is reasonable to assume that the reaction

Table 1
Main reflections (normalized/measured intensities) observed during the $VOHPO_4 \cdot 0.5H_2O \rightarrow \alpha$-$(NH_4)_2[(VO)_3(P_2O_7)_2]$ transformation, processing during toluene ammoxidation. $VOHPO_4 \cdot 0.5H_2O$ was heated up to 673 K (heating rate $\beta = 10$ K/min) under a feed with molar ratios of toluene:air:$NH_3$:$H_2O$ = 1:30:5:25 and held for different periods of time. Afterwards, XRD data for the different samples were taken

| 2Θ (°) | 15.6 | 15.8 | 16.4 | 24.0 | 27.1 | 30.44 |
|---|---|---|---|---|---|---|
| $VOHPO_4 \cdot 0.5H_2O$ | 52/2449 | | | | 41/1927 | 100/4756 |
| 0.25 h | 42/697 | | | | 11/183 | 100/1642 |
| 0.5 h | | | | | | 100/114 |
| 2 h | | | | 100/84 | | |
| 6 h | | 100/624 | 57/358 | 91/567 | | |
| 10 h | | 100/1529 | 68/1038 | 71/1080 | | |
| $NVPO_{syn}$ | | 100/6569 | 74/4848 | 79/5183 | | |

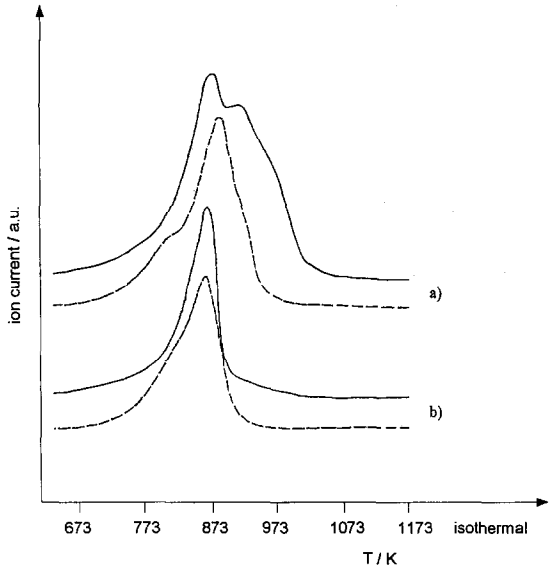


Fig. 2. Ion current profiles of (a) $H_2O$ (m/e 18) and (b) $NH_3$ (*m/e* 15) liberation during temperature-programmed reaction in a flow of He (heating rate $\beta = 4$ K/min); full line $\alpha$-$(NH_4)_2[(VO)_3(P_2O_7)_2]$, $NVPO_{syn}$; dashed line $\alpha$-$(NH_4)_2[(VO)_3(P_2O_7)_2] + V_xO_y$, $NVPO_{aox}$.

product $V_9^{IV}O_{45}P_{12}N_2$ is a mixture of a nitrido phosphate $(V^{IV}O)_3[(P_3O_9)N]$ and a polyphosphate $V^{IV}O(PO_3)_2$. Thus Eq. (2) can be specified by Eq. (3):

$$3\alpha\text{-}(NH_4)_2\left[(V^{IV}O)_3(P_2O_7)_2\right] \Rightarrow 2(V^{IV}O)_3\left[(P_3O_9)N\right] + 3V^{IV}O(PO_3)_2 + 6H_2O + 4NH_3 \quad (3)$$

The $N_2$ formation upon heating of $NVPO_{syn}$ and $NVPO_{aox}$ is demonstrated in Fig. 3. Small amounts of $N_2$ were obtained in the temperature range of $NH_3$ desorption (see Fig. 2) caused by partial oxidation of formed $NH_3$. The liberation of the main portion of $N_2$ above 973 K is due to the thermal decomposition of the nitrido phosphate phase according to Eq. (4):

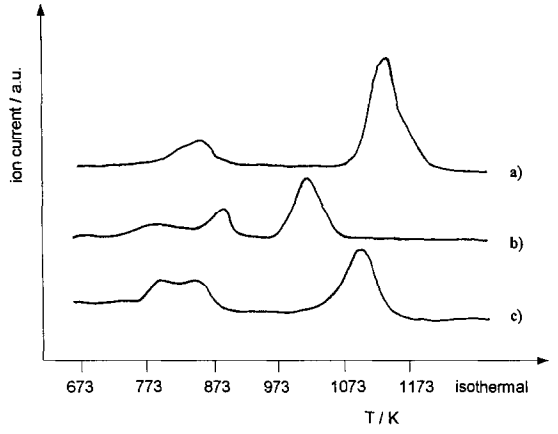


Fig. 3. Desorption of $N_2$ (*m/e* 28) formed during temperature-programmed decomposition in a flow of He (heating rate $\beta = 4$ K/min); (a) $\alpha$-$(NH_4)_2[(VO)_3(P_2O_7)_2]$, $NVPO_{syn}$; (b) $\alpha$-$(NH_4)_2[(VO)_3(P_2O_7)_2] + V_xO_y$, $NVPO_{aox}$; (c) $\alpha$-$(NH_4)_2[(VO)_3(P_2O_7)_2] + NH_4VO_3$, $NVPO_{syn/m}$.

$$2(V^{IV}O)_3\left[(P_3O_9)N\right] \Rightarrow V_4^{III}(P_2O_7)_3 + N_2 + V_2^{III}O_3 \quad (4)$$

The formation of $V_4^{III}(P_2O_7)_3$ was proven by comparison of the XRD patterns with that of a synthesized sample of $V_4^{III}(P_2O_7)_3$. The onset of the $N_2$ formation during heating of $NVPO_{aox}$ occurred at a significantly lower temperature than in the case of $NVPO_{syn}$. The analogous experiment with $NVPO_{syn/m}$ showed a shift of the $N_2$ peak towards lower temperatures in comparison to $NVPO_{syn}$, too. $NH_4VO_3$ is transformed to disperse $V_2O_5$ at above 423 K [10]. The observed shift of the temperature of the $N_2$ liberation indicates an interaction of $V_xO_y$ with $NVPO_{syn}$ or $(V^{IV}O)_3[(P_3O_9)N]$ formed from $NVPO_{syn}$ at least. Obviously, $V_xO_y$ promotes the redox decomposition of the nitrido phosphate phase.

Table 2
Catalytic properties of $(VO)_2P_2O_7$, $NVPO_{syn}$, $NVPO_{aox}$ and $NVPO_{syn/i}$ during the ammoxidation of toluene. Conditions: quartz glass U-tube reactor; 1.5 ml catalyst; $W/F = 9$ g h mol$^{-1}$; molar ratios toluene:air:$NH_3$:$H_2O$ = 1:30:5:25; normal pressure

| Sample | $(VO)_2P_2O_7$ | $NVPO_{syn}$ [a] | $NVPO_{aox}$ [b] | $NVPO_{syn/i}$ |
|---|---|---|---|---|
| $T$ (K) | 673 | 713 | 678 | 623 |
| Toluene conversion (mol%) | 22 | 21 | 25 | 27 |
| Nitrile selectivity (%) | 73 | 99 | 80 | 78 |

[a] BET surface area: 5 $m^2/g$.
[b] BET surface area: 2.5 $m^2/g$.

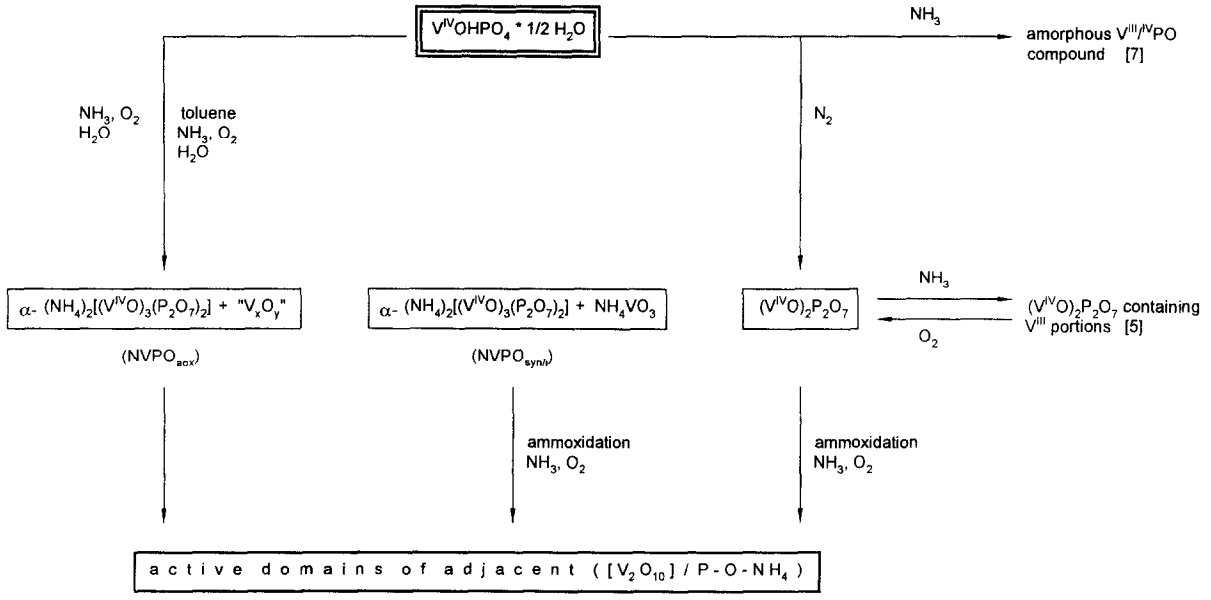


Scheme 1.

Therefore, we assume that the $V_xO_y$ phase could also act as oxygen transfer compound during the ammoxidation of methylaromatics over the catalyst sample $NVPO_{aox}$. The results of catalytic testing of $(VO)_2P_2O_7$, $NVPO_{syn}$, $NVPO_{aox}$ and $NVPO_{syn/i}$ are demonstrated in Table 2. $(VO)_2P_2O_7$ and $NVPO_{aox}$ showed comparable activity and nitrile selectivity, whereas a significant higher temperature was necessary to obtain a similar activity with $NVPO_{syn}$. The activity differences of both catalysts are strengthened taking into account their different BET surface areas ($NVPO_{aox} = 2.5$ $m^2/g$; $NVPO_{syn} = 5$ $m^2/g$. Otherwise, the activity of $NVPO_{syn}$ was essentially increased by vanadium oxide generated from $NH_4VO_3$ marked by the possible lowering of the reaction temperature. This effect could be interpreted by the formation of active domains according to the 'coherent interfacial model' [11] as well as by the concept of 'remote control' (e.g. [12]).

## 4. Conclusions

The reactions taking place during interaction of $VOHPO_4 \cdot 0.5H_2O$ and $(VO)_2P_2O_7$, respectively, with feed components of the ammoxidation reaction are summarized in Scheme 1. Scheme 1 includes the formation of an active catalyst consisting of $\alpha$-$(NH_4)_2[(VO)_3(P_2O_7)_2]$ impregnated with $NH_4VO_3$.

$VOHPO_4 \cdot 0.5H_2O$ is transformed in different ways depending on whether it is heated in inert gas, $NH_3$, $NH_3/O_2$, $NH_3/O_2/H_2O$ or under the water containing ammoxidation feed [7]. As well known, heating of $VOHPO_4 \cdot 0.5H_2O$ under inert gas leads to $(VO)_2P_2O_7$ whereas by interaction with $NH_3$ an XRD-amorphous $V^{III}$-containing product is generated comparable to the phase formed partially upon reductive interaction of $NH_3$ with $(VO)_2P_2O_7$. Otherwise, a partial transformation of $VOHPO_4 \cdot 0.5H_2O$ to a crystalline NVPO structure is observed in the presence of an $NH_3/O_2$ mixture. Obviously, the presence of $O_2$ prevents the formation of the amorphous $V^{III}$-containing product. However, as can be observed in the case of heating in a flow of $NH_3/O_2/H_2O$ or under ammoxidation conditions, water is needed for a complete transformation of $VOHPO_4 \cdot 0.5H_2O$ to the $NVPO_{aox}$ phase because only in these cases a well crystalline product was observed.

One could suggest that a mixed valent vanadium oxide phase ($V_xO_y$ phase of $NVPO_{aox}$ or mainly $V_2O_5$ generated by the metavanadate decomposition of $NVPO_{syn/i}$) could modify the catalytic properties of $\alpha$-$(NH_4)_2[(VO)_3(P_2O_7)_2]$ in two different ways. On the one hand, such a vanadium oxide phase could supply selective oxidizing species to $\alpha$-$(NH_4)_2[(VO)_3(P_2O_7)_2]$ according to the 'remote control' concept [12]. On the other hand, $[V_2O_{10}]$ double octahedra could be embedded into surface layers of $\alpha$-$(NH_4)_2[(VO)_3(P_2O_7)_2]$ or cover its surface, forming active domains ('coherent interfacial model' [11]). $[V_2O_{10}]$ of the (100) plane of $(VO)_2P_2O_7$ are considered to be sites for adsorption of methylaromatics as well as ammonia [8]. This structural unit and the surrounding acid P-OH groups, generating ammonium ions under ammoxidation conditions, are probably responsible for O- as well as N-insertion, forming nitriles via aldehyde intermediates. Therefore, we suggest the presence of similar structural elements, namely domains of adjacent $[V_2O_{10}]$ double octahedra and P-O-$NH_4$ groups on the surface of $NVPO_{aox}$ and $(VO)_2P_2O_7$.

This conception would explain the very similar catalytic properties of different VPO-materials in the ammoxidation reaction discussed above. However, this interpretation needs further investigations concerning the kind of interaction of both phases being present in the ammoxidation catalyst $NVPO_{aox}$ formed from the precursor $VOHPO_4 \cdot 0.5H_2O$, particularly.

## Acknowledgements

The authors gratefully acknowledge the Bundesminister für Bildung, Wissenschaft, Forschung und Technologie (project 423-4003-03D0001B0) for financial support.

## References

[1] G. Centi, Editor, Catal. Today, 16 (1993).
[2] A. Martin, B. Lücke, H. Seeboth and G. Ladwig, Appl. Catal., 49 (1989) 205.
[3] A. Martin, B. Lücke, H. Seeboth, G. Ladwig and E. Fischer, React. Kinet. Catal. Lett., 38 (1989) 33.
[4] B. Lücke and A. Martin, in M.G. Scaros and M.L. Prunier, Editors, Catalysis of Organic Reactions, Marcel Dekker, New York, 1995, p. 479.
[5] H. Berndt, K. Büker, A. Martin, A. Brückner and B. Lücke, J. Chem. Soc., Faraday Trans., 91 (1995) 725.
[6] A. Martin, B. Lücke, G.-U. Wolf and M. Meisel, Catal. Lett., 33 (1995) 349.
[7] Y. Zhang, A. Martin, G.-U. Wolf, S. Rabe, H. Worzala, B. Lücke, M. Meisel and K. Witke, Chem. Mater. 8 (1996) 1135.
[8] A. Martin, H. Berndt, B. Lücke and M. Meisel, Topics Catal., in press.
[9] R. Conanec, W. Feldmann, R. Marchand and Y. Laurent, J. Solid State Chem. 121 (1996) 418.
[10] C. Lampe-Önnerud and J.O. Thomas, J. Mater. Chem., 5 (1995) 1075.
[11] E. Bordes, Catal. Today, 1 (1987) 499.
[12] L.-T. Weng and B. Delmon, Appl. Catal. A: General, 81 (1992) 141.